# Electronic Supplementary Information

## Highly sensitive capacitance-based nitrite sensing using polydopamine/AuNPs-modified screen-printed carbon electrode.

Faisal K. Algethami,[a]*Amal Rabti,[b,c] Mohamed Mastouri,[b] Babiker Y. Abdulkhair[a], Sami Ben Aoun,[d] and Noureddine Raouafi[c]*

[a]Department of Chemistry, College of Science, Imam Mohammad Ibn Saud Islamic University, P.O. Box 90950, Riyadh 11623, Saudi Arabia.

[b]National Institute of Research and Physicochemical Analysis (INRAP), Laboratory of Materials, Treatment, and Analysis (LMTA), Biotechpole Sidi Thabet, 2020 Sidi Thabet, Tunisia.

[c]Sensors and Biosensors Group, Analytical Chemistry and Electrochemistry Lab (LR99ES15), University of Tunis El Manar, Tunis El Manar, 2092 Tunis, Tunisia.

[d]Department of Chemistry, Faculty of Science, Taibah University, P.O Box 30002, Al-Madinah Al-Munawwarah, Saudi Arabia.

*Corresponding author Email: noureddine.raouafi@fst.utm.tn (Noureddine Raouafi), falgethami@imamu.edu.sa (Faisal K. Algethami).

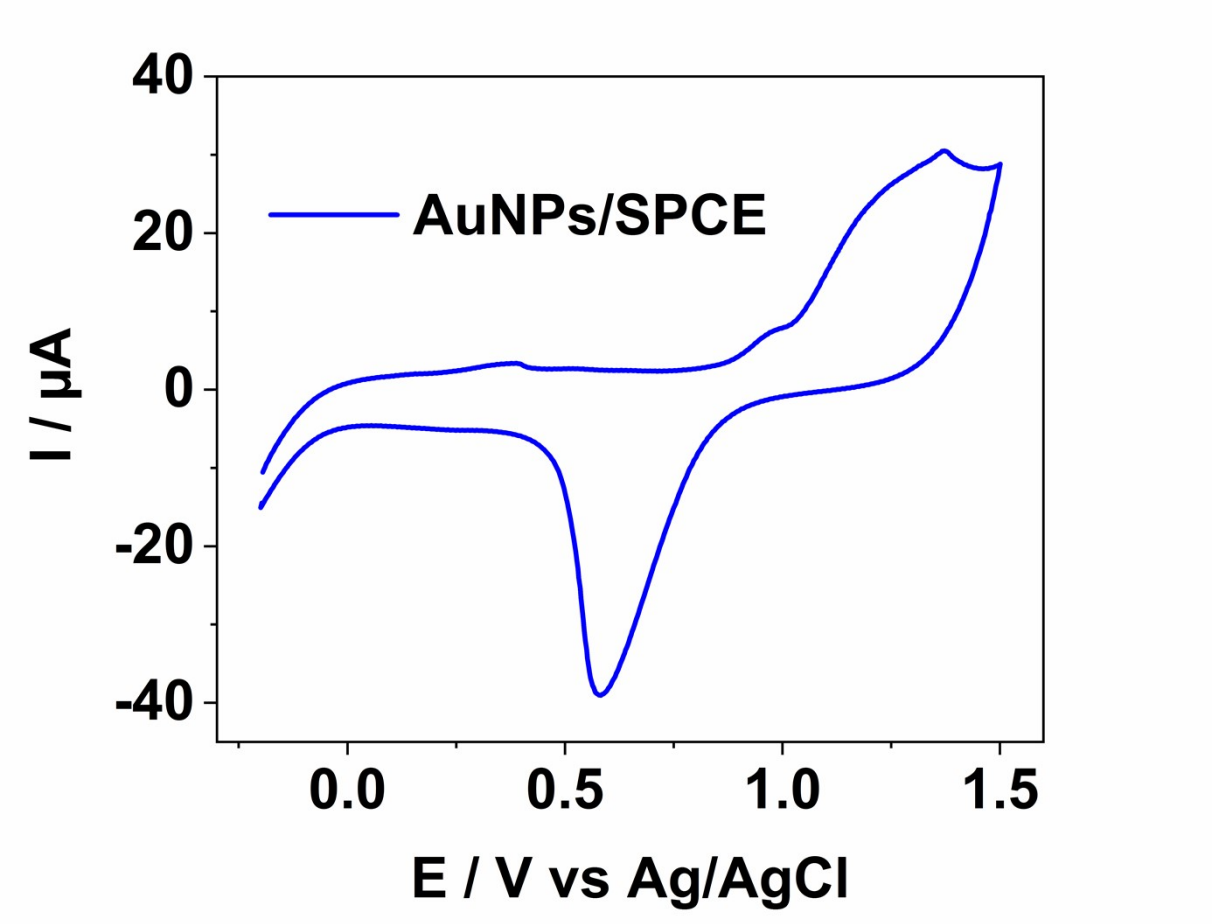


**Figure S1.** CV responses of AuNPs/SPCE in 0.5 M $H_2SO_4$ solution at the scan rate of 0.1 $V \cdot s^{-1}$.

## Surface area determination

In order to calculate the surface area of SPCE, AuNPs/SPCE and pDA/AuNPs/SPCE, CVs of 5.0 mM $[Fe(CN)_6]^{3/4-}$ (the diffusion coefficient $D = 6.7 \times 10^{-6}$ $cm^2 \cdot s^{-1}$) were recorded. Using Randles–Sevcik equation (Eq. 1):

$$i_p = 2.69 \times 10^5 \, n^{3/2} \, A \, D^{1/2} \, v^{1/2} \, C \qquad \text{(Eq. 1)}$$

Where n is the number of electrons involved in the redox reaction, A is the effective area ($cm^2$), D is the diffusion coefficient of the redox molecule in solution ($cm^2 \cdot s^{-1}$), v is the scan rate ($V \cdot s^{-1}$) and C is the bulk concentration of the probe molecule, the effective surface area of the SPCE, AuNPs/SPCE and pDA/AuNPs/SPCE were estimated to be 0.045 $cm^2$, 0.048 $cm^2$ and 0.051 $cm^2$, respectively. The increases of active surface areas compared to bare SPCE were 8 % and 13 % for AuNPs/SPCE and pDA/AuNPs/SPCE, respectively, demonstrating the higher electrochemical activity of the modified electrodes.

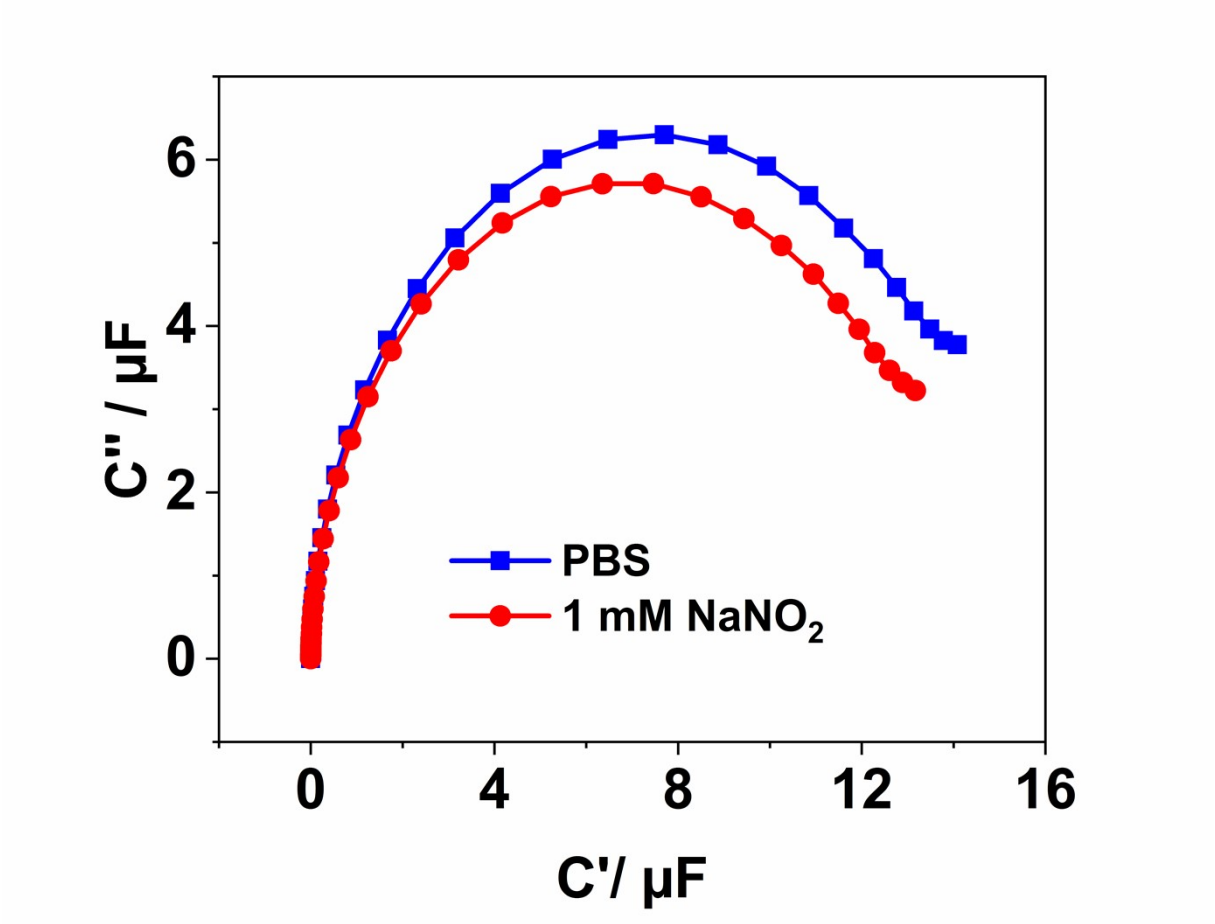


**Figure S2.** Capacitance Nyquist plots of AuNPs/SPCE in the absence and presence of 1 mM $NaNO_2$ in 0.01 M PBS (pH 7.0).

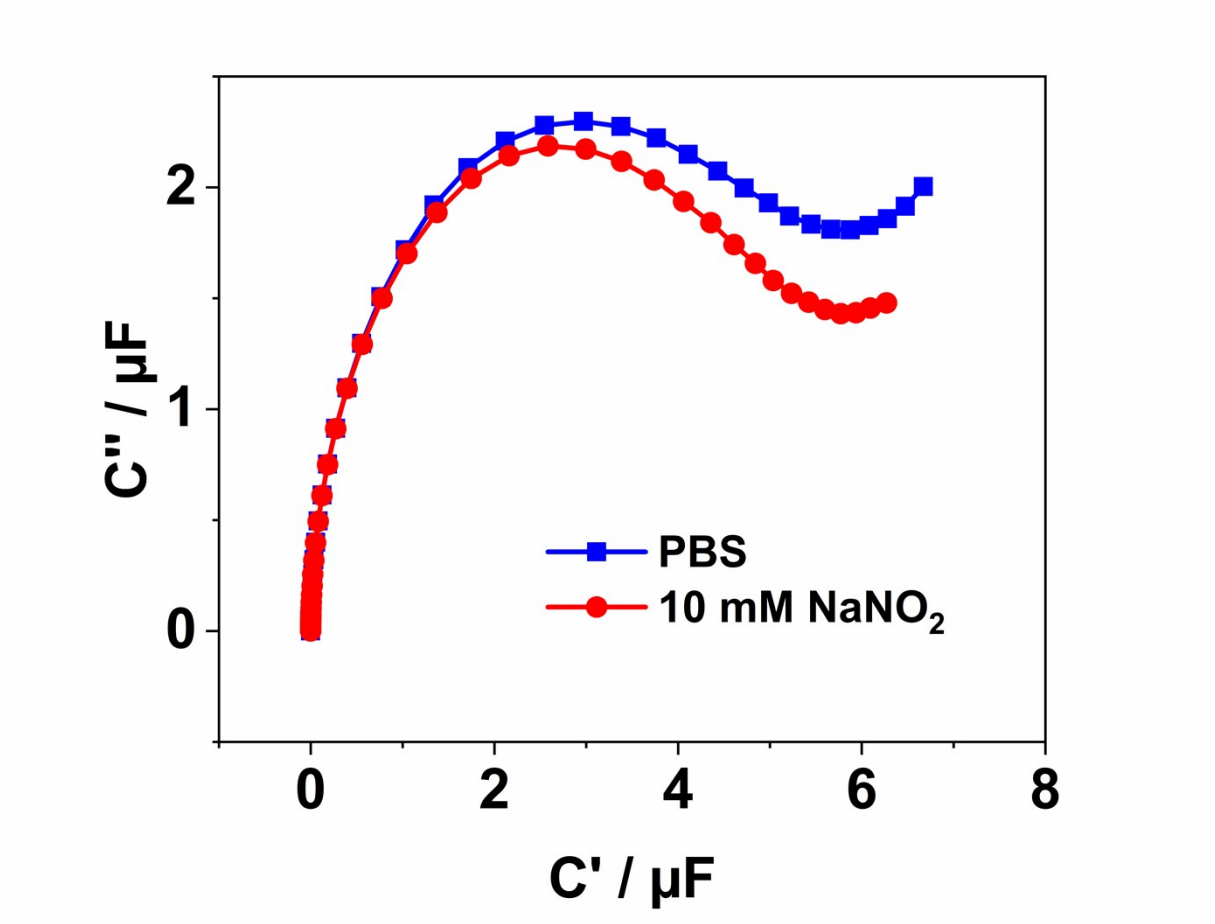


**Figure S3.** Capacitance Nyquist plots of PDA/SPCE in the absence and presence of 1 mM $NaNO_2$ in 0.01 M PBS (pH 7.0).

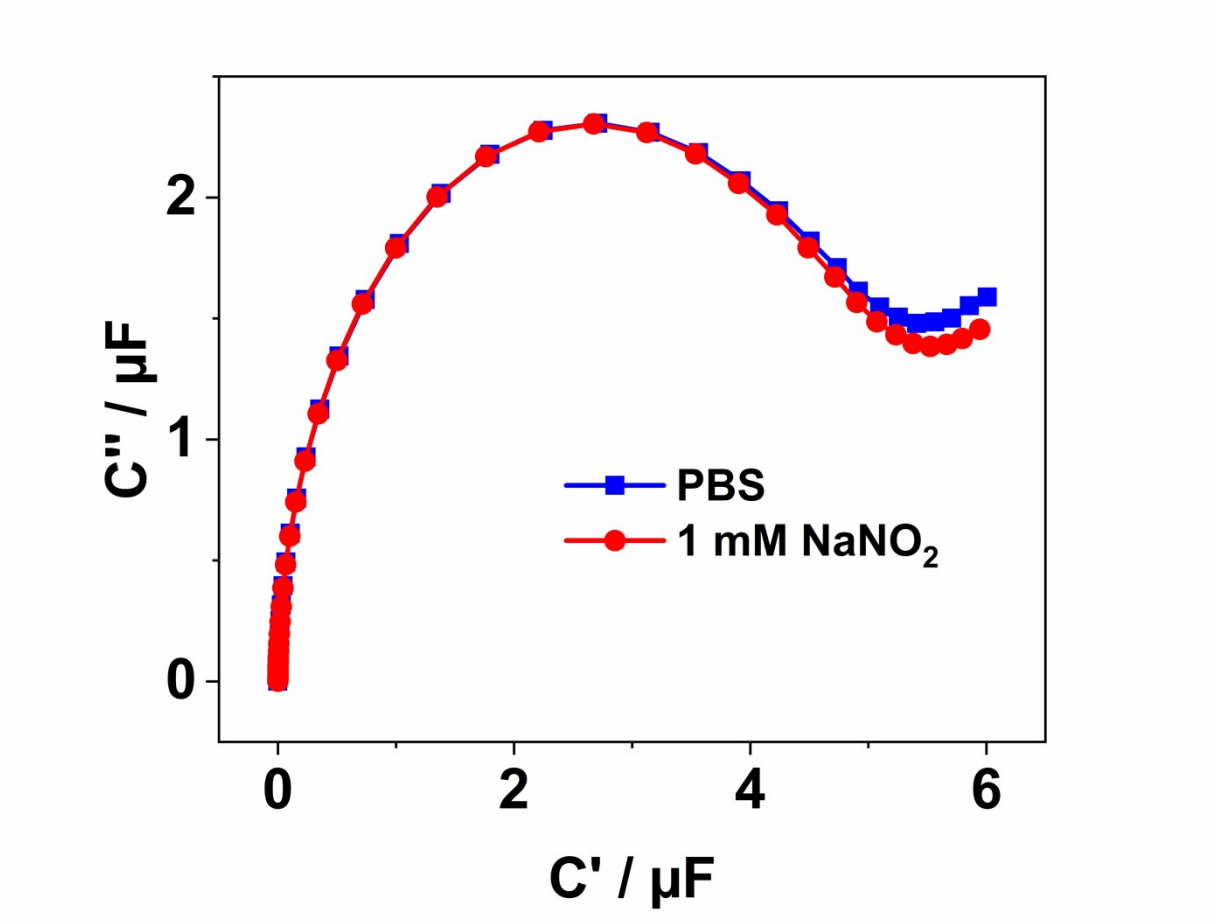


**Figure S4.** Capacitance Nyquist plots of SPCE in the absence and presence of 1 mM $NaNO_2$ in 0.01 M PBS (pH 7.0).

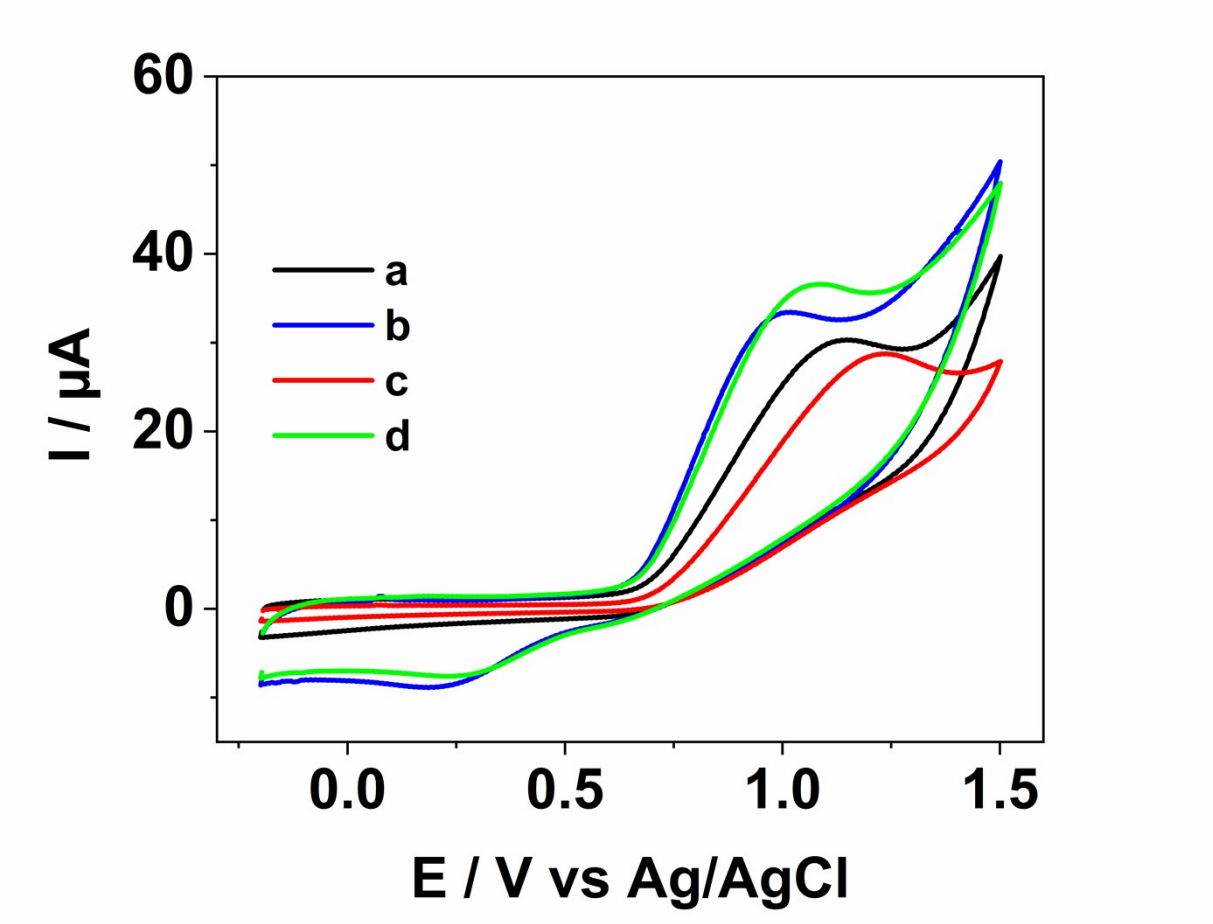


**Figure S5.** CVs of (a) SPCE, (b) AuNPs/SPCE, (c) pDA/SPCE and (d) pDA/AuNPs/SPCE in the presence of 1 mM $NaNO_2$ at a scan rate of 100 $mV \cdot s^{-1}$ in 0.01 M PBS (pH 7.0).

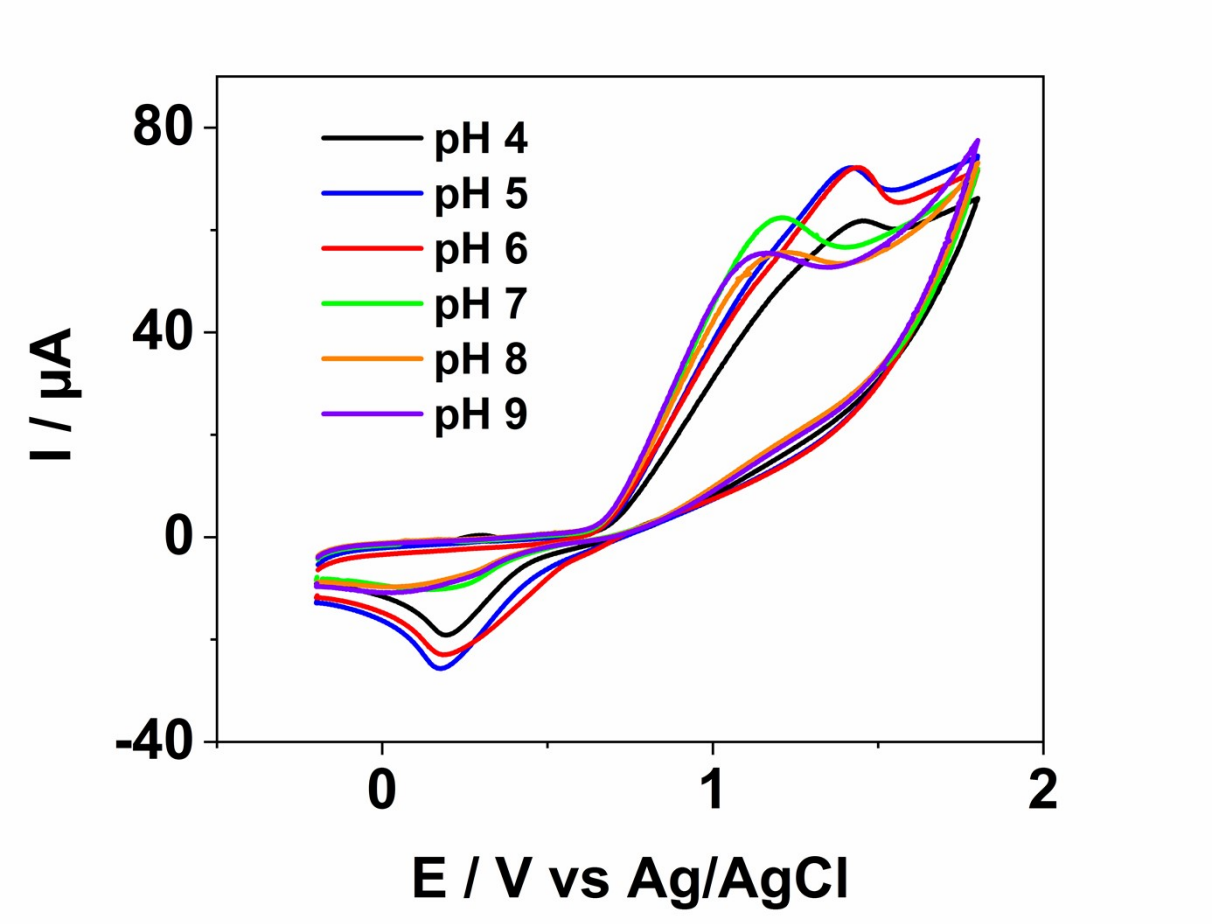


**Figure S6.** CVs of pDA/AuNPs/SPCE SPCE in the presence of 1 mM $NaNO_2$ at a scan rate of 100 $mV \cdot s^{-1}$ in 0.01 M PBS at different pH.

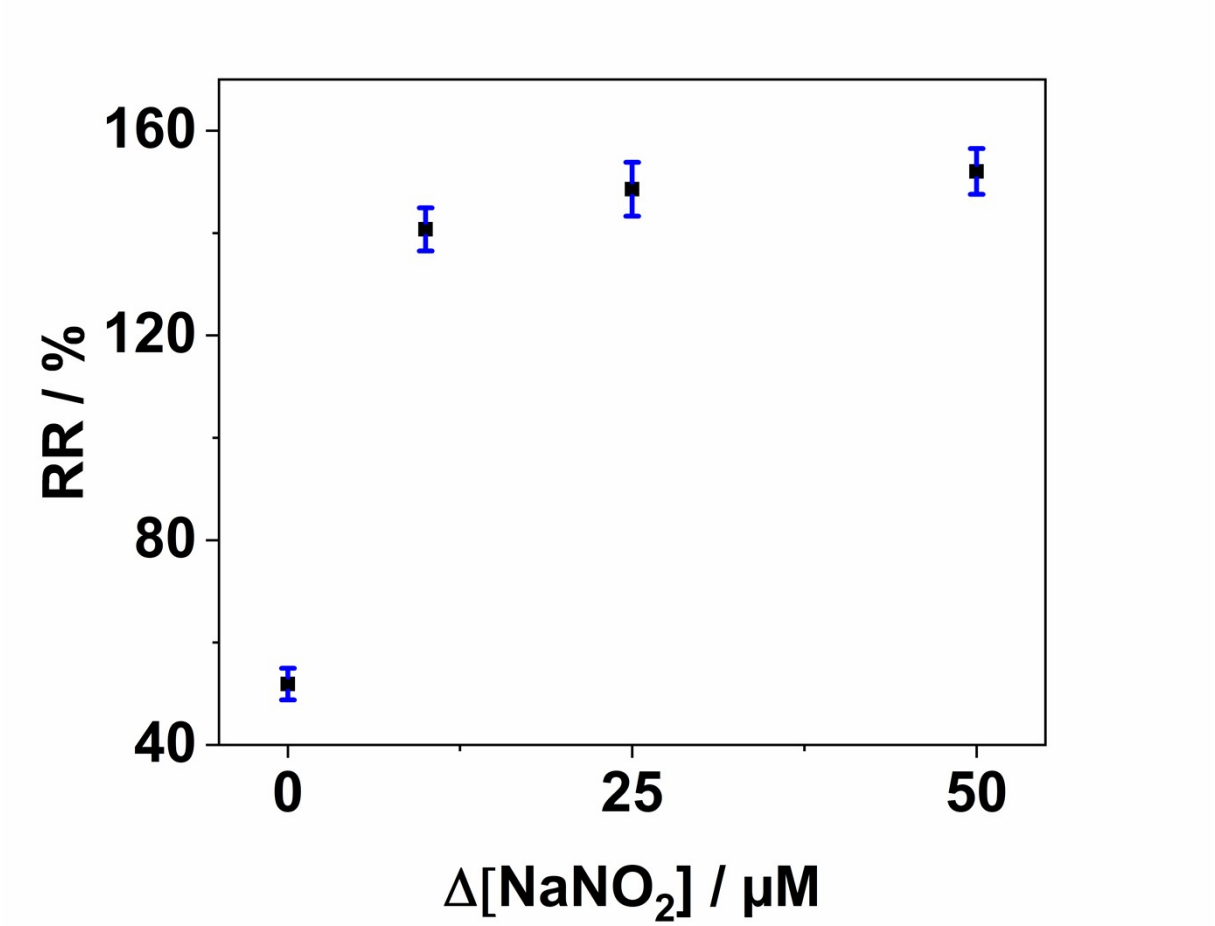


**Figure S7.** The relative variation of redox capacitance RR% vs. $\Delta[NO_2^-]$ obtained in salami spiked samples.

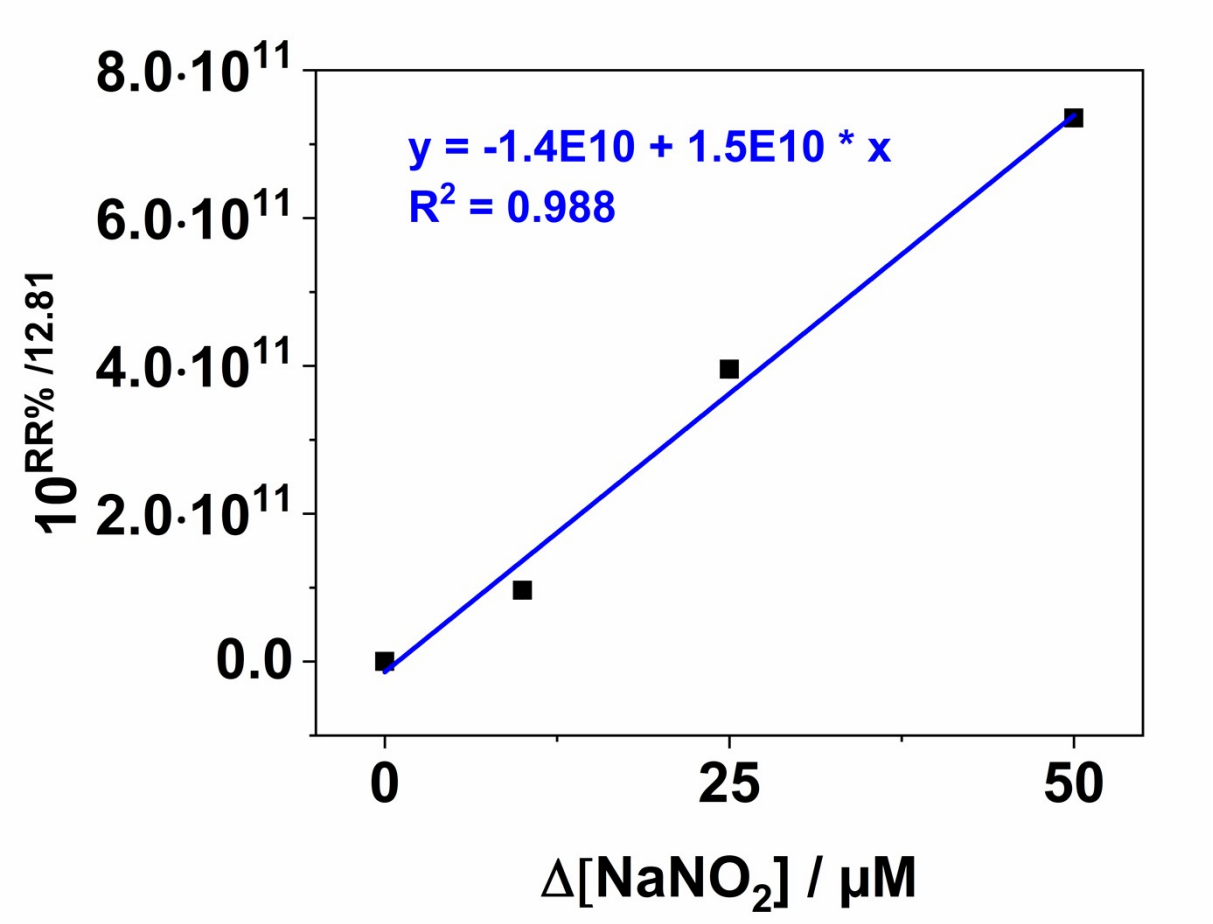


**Figure S8.** Graph of the proposed standard addition method application for nitrite determination in salami sample.